

# Comparative analysis of dosimetric and radiobiological models of IPSA and HIPO algorithms in combined intra-cavitary/interstitial brachytherapy for cervical cancer

Chuanjun Yan, MS<sup>1</sup>, Xianliang Wang, PhD<sup>2</sup>, Aiping Wen, MS<sup>3</sup>, Jingyue Luo, MSc<sup>2</sup>, Siyu Zhang, MS<sup>3</sup>, Pei Wang, MSc<sup>2</sup>, Jie Li, MSc<sup>1,2</sup>

<sup>1</sup>School of Medicine, Southwest Medical University of China, Luzhou, Sichuan Province, China, <sup>2</sup>Department of Radiotherapy, Radiation Oncology Key Laboratory of Sichuan Province, Sichuan Clinical Research Center for Cancer, Sichuan Cancer Hospital & Institute, Sichuan Cancer Center, Affiliated Cancer Hospital of University of Electronic Science and Technology of China, Chengdu, China, <sup>3</sup>School of Medicine, University of Electronic Science and Technology of China, Chengdu, Sichuan Province, China

## Abstract

**Purpose:** To compare inverse planning simulated annealing (IPSA) and hybrid inverse planning optimization (HIPO) using dosimetric and radiobiological models, and provide a basis for selecting the optimization method for cervical cancer.

**Material and methods:** This was a retrospective study including 32 patients with radical cervical cancer. Brachytherapy treatment plans were re-optimized using IPSA, HIPO1 (with a locked uterine tube), and HIPO2 (with an unlocked uterine tube). Dosimetric data, including isodose lines, HR-CTV ( $D_{100}$ ,  $V_{150\%}$ ,  $V_{200\%}$ , HI, and CI), and (bladder, rectum, and intestines)  $D_{1cc}$ ,  $D_{2cc}$  for organs at risk (OARs) were also collected. Additionally, TCP, NTCP, BED, and EUBED were calculated, and differences were analyzed using matched samples *t*-test and Friedman test.

**Results:** Compared with IPSA and HIPO2, HIPO1 had better  $V_{150\%}$  and  $V_{200\%}$  ( $p < 0.05$ ). Compared with IPSA and HIPO1, HIPO2 had better  $D_{100}$  and CI ( $p < 0.05$ ). The doses to the bladder  $D_{1cc}$  ( $4.72 \pm 0.33$  Gy)/ $D_{2cc}$  ( $4.47 \pm 0.29$  Gy) and rectum  $D_{1cc}$  ( $4.50 \pm 0.61$  Gy)/ $D_{2cc}$  ( $4.11 \pm 0.63$  Gy) were lower in HIPO2 than in IPSA and HIPO1. EUBEDs for HR-CTV were higher in HIPO1 and HIPO2 than in IPSA by 1.39-1.63%. However, TCPs were not remarkably different among the three plans ( $p > 0.05$ ). Also, the NTCP for the bladder was lower in HIPO2 than in IPSA and HIPO1 by 13.04% and 16.67%, respectively.

**Conclusions:** Although the dosimetric parameters of IPSA, HIPO1, and HIPO2 are comparable, HIPO2 provides better dose conformability and lower NTCP. Therefore, HIPO2 is recommended as an optimization algorithm in IC/ISBT for cervical cancer.

J Contemp Brachytherapy 2023; 15, 3: 212-219

DOI: <https://doi.org/10.5114/jcb.2023.128894>

**Key words:** cervical cancer, intra-cavitary/interstitial brachytherapy, IPSA, HIPO, EUBED, TCP/NTCP.

## Purpose

Brachytherapy (BT) is performed by directly placing the radiation source in or near the tumor site [1]. Brachytherapy plays an essential role in treating cervical cancer. Cervical cancer is a common malignant tumor in females, which seriously threatens women's health [2]. External beam radiation therapy (EBRT) combined with intra-cavitary brachytherapy (ICBT) is widely used for cervical cancer treatment. However, ICBT provides a lower target coverage when the tumor is bulky, obliterated, or if there is vaginal stenosis or disappearing of vaginal vault, resulting in poorer outcomes [3]. None-

theless, interstitial brachytherapy (ISBT) combined with ICBT (IC/ISBT) can compensate the disadvantages of ICBT by increasing the dose coverage of clinical target volume (CTV) [4]. The methods for optimizing IC/ISBT mainly consist of graphical optimization and inverse optimization. Inverse optimization methods include inverse planning simulated annealing (IPSA), hybrid inverse planning optimization (HIPO), gradient-based planning optimization (GBPO), GPU-based multi-criteria optimization (gMCO), etc. [5, 6].

Inverse planning simulated annealing reduces the dose to organs at risk (OARs) while increasing the target-dose coverage during cervical cancer treatment with

**Address for correspondence:** Jie Li, MSc, School of Medicine, Southwest Medical University of China, Department of Radiotherapy, Radiation Oncology Key Laboratory of Sichuan Province, Sichuan Clinical Research Center for Cancer, Sichuan Cancer Hospital & Institute, Sichuan Cancer Center, Affiliated Cancer Hospital of University of Electronic Science and Technology of China, No. 55, 4<sup>th</sup> Section, Renmin South Road, Chengdu, Sichuan Province, 610041, China, phone: +86 13880270250, e-mail: [jie.li@yeah.net](mailto:jie.li@yeah.net)

Received: 16.09.2022  
Accepted: 04.04.2023  
Published: 23.06.2023

BT [6-8]. Kim *et al.* [9] and Tinkle *et al.* [10] found that IPSA has good tolerance and low toxicity, and thus achieves a reasonable local control. Hybrid inverse planning optimization has been widely used in the treatment of cervical cancer and other cancers with BT [11-13]. Trnková *et al.* [14] concluded that HIPO can eliminate high-dose regions in normal tissue. Fu *et al.* [15] also showed that the dwell-time distribution produced by HIPO may better match clinical preferences than that produced by IPSA.

Although studies have assessed IPSA and HIPO-based dosimetric perspective, no research has assessed IPSA and HIPO in IC/ISBT for cervical cancer based on radiobiological perspective. Therefore, additional parameters about tumor control probability (TCP) and normal tissue complication probability (NTCP) are expected to make the clinicians to evaluate plans more thoroughly and determine their potential advantages in clinical application. This study aimed to compare IPSA and HIPO from dosimetric and radiobiological perspectives.

## Material and methods

### Patients

We retrospectively analyzed data of 32 cervical cancer patients who received radical therapy in our hospital from January, 1 to October, 31, 2021. An ethics approval was obtained to include available data in the study. Patients with squamous cell carcinoma were aged between 30 and 77 years. Stages ranged from IB<sub>2</sub> to IV<sub>A</sub> according to the 2018 staging of the Federation of Gynecology and Obstetrics (FIGO) classification [16].

### Treatment methods

Patients underwent EBRT and IC/ISBT with or without chemotherapy. Target doses of EBRT and BT were 45 Gy/25 fractions and 30 Gy/5 fractions, respectively. Each IC/ISBT treatment plan for each patient was evaluated separately. BT was performed in an operating room under general anesthesia. A Foley catheter was placed in the bladder, and 7 cc opaque contrast agent was injected in the balloon. Experienced clinicians preliminarily determined the tumor location, size, shape, and invasion using either MRI or CT before BT. A gynecological examination

was also conducted before BT. A Fletcher intra-cavity applicator (intra-uterine tube Elekta, part No. 189.739; Stockholm, Sweden) and interstitial needles (range, 4-8 needles; ProGuide plastic needles, Elekta part No. 189.601) were applied for the BT process. A 3D-printed multi-channel vaginal applicator was used for guidance of needle implantation and fixation of the intra-uterine tube. Patients were transported to CT (Brilliance Big Bore CT, produced by Philips, The Netherlands) room to complete localization scan. Scanning range of CT was from the anterior superior iliac ridge to the lower edge of ischial tuberosity. Slice thickness was 3 mm. The image was imported to Oncentra Brachy v. 4.3 treatment planning system (TPS) (Elekta AB). Clinicians delineated HR-CTV and OARs following the recommended standards of the International Commission on Radiation Units (ICRU) (Report No. 89 [17]).

### Planning objectives

Treatment plan was performed using Oncentra Brachy TPS. Applicator reconstructions were based on ICRU recommendations [17], and the source stepping size was 5 mm. Offset value of metal uterine tube and interstitial needle value were -0.6 cm and -0.35 cm, respectively [18]. Brachytherapy plan for the first IC/ISBT fraction of each patient was compared. A total of 96 BT plans were created for all patients (each patient had three plans: IPSA, HIPO1, and HIPO2). IPSA employs a fast randomized simulated-annealing algorithm, which takes into account anatomical geometry to optimize source dwell times [19-22]. Optimization process takes less than 1 minute. HIPO combines stochastic simulated-annealing algorithm with a limited-memory Broyden-Fletcher-Goldfarb-Shanno (L-BFGS) deterministic algorithm for three-dimensional (3D) dose-distribution optimization. Manual source position activation and partial catheter optimization are allowed in HIPO [23]. In this study, IPSA, HIPO1, and HIPO2 were completed with the same constraints for anatomical structure of the target area (Table 1). HIPO1 involved maximizing the contribution of uterine tube and locking the uterine tube before optimization, while the uterine tube was not locked and optimized directly under the same initial objectives in HIPO2. Dwell-time deviation constraint (DTDC) and

**Table 1.** Optimization objectives used for IPSA, HIPO1, and HIPO2

Optimization method	Organ	Minimum dose (Gy)	Weight	Maximum dose (Gy)	Weight
IPSA	HR-CTV (surface)	6	100		
	Bladder (surface)			4	100
	Intestines (surface)			4	100
	Rectum (surface)			4	100
HIPO	HR-CTV (surface)	6	100	12	1
	Bladder (surface)			4	100
	Intestines (surface)			4	100
	Rectum (surface)			4	100
	Normal tissue (surface)			12	1

HR-CTV – high-risk clinical target volume, IPSA – inverse planning simulated annealing, HIPO – hybrid inverse planning optimization

dwell-time gradient restriction (DTGR) of IPSA, HIPO1, and HIPO2 were 0.6. The objective parameters (without graphical optimization) were continuously adjusted to ensure that HR-CTV  $D_{90}$  of all patients reached 6 Gy (difference: less than 0.01 Gy), while OARs' dose was as low as possible. All plans were calculated for a standardized source strength  $S_k$  of  $1.6136 \times 10^{-2} \text{ Gy}\cdot\text{m}^2\cdot\text{h}^{-1}$  for iridium-192 ( $^{192}\text{Ir}$ ) source.

**Dosimetric indexes and data analysis**

Dosimetric indexes included isodose lines; HR-CTV  $D_{100}$ ,  $V_{150\%}$ ,  $V_{200\%}$ , homogeneity index (HI), and conformity index (CI);  $D_{1cc}/D_{2cc}$  for OARs (bladder, rectum, and intestines); and TCP, NTCP, biologically effective dose (BED), and equivalent uniform biologically effective dose (EUBED).  $D_x$  was defined as the irradiation dose received by the x% relative volume or the x cm<sup>3</sup> absolute volume.  $V_{y\%}$  was defined as the volume percentage of the prescription dose of y%.

**HI and CI calculations**

HI [24] was calculated as follows:

$$HI = \frac{V_{100\%} - V_{150\%}}{V_{100\%}} \tag{1}$$

CI [25] was calculated as follows:

$$CI = \frac{V_{T,ref}}{V_T} \times \frac{V_{T,ref}}{V_{ref}} \tag{2}$$

Where  $V_{T,ref}$  is the volume of HR-CTV covered by the prescribed isodose (cm<sup>3</sup>);  $V_T$  and  $V_{ref}$  are the volume of HR-CTV (cm<sup>3</sup>) and volume of the prescribed isodose (cm<sup>3</sup>), respectively.

**TCP and NTCP calculations**

Tumor dose was not uniform in BT. Niemierko proposed the concept of equivalent uniform dose (EUD) [26] [27], as follows:

$$EUD = \left( \sum_{i=1}^N (V_i D_i^a) \right)^{\frac{1}{a}} \tag{3}$$

Where  $V_i$  is the part of the target volume that is irradiated by a dose ( $D_i$ );  $D_i$  is the dose received by the voxel volume at  $i$ , and  $a$  is the parameter that describes the dose-volume effect of tumor or normal tissue.

In this study, a value used was adopted from reference [28, 29] as shown in Table 2.  $a = +\infty$ ,  $a = -\infty$ ,  $a = 1$ , and  $a = 0$  indicated maximum dose, minimum dose, average dose, and geometric mean dose, respectively [30]. Local control of the tumor may depend on the minimum dose volume because this is the spot where the survival rate of

tumor clones is the highest. Therefore,  $a$  should be a large negative value in the tumor. However,  $a$  should be a large positive value in normal tissues with tandem structures.

Niemierko proposed the TCP/NTCP model based on the concept of EUD as follows [27]:

$$TCP = \frac{1}{1 + \left( \frac{TCD_{50}}{EUD} \right)^{4\gamma_{50}}} \tag{4}$$

$$NTCP = \frac{1}{1 + \left( \frac{TD_{50}}{EUD} \right)^{4\gamma_{50}}} \tag{5}$$

Where  $TCD_{50}$  is the 50% efficiency dose and  $\gamma$  is the parameter that describes the characteristics of the dose-response curve.  $\gamma$  is related to the steepness of the dose-response curve (normalized steepness of the dose-response curve).  $\gamma_{50}$  is the value of the dose-response curve ( $\gamma$ ) at the point of  $TCP = 0.5$  and  $D = D_{50}$ .  $TD_{50}$  is the dose required for a 50% probability of complications to an organ caused by radiation on the whole volume.

In the present study, the published code of Gay *et al.* for calculating TCP/NTCP [29] was applied. These formulas take into account the total dose of radiotherapy. TCP and NTCP were predicted and evaluated based on a single treatment. Nesvacil *et al.* [31] proposed the formula below, where  $d_i$  represents the dose of voxel  $i$  in a single treatment.  $D_i$  is denoted by (EBRT 45 Gy + IC/ISBT  $d_i \times 5$  fractions):

$$D_i = 45 + d_i \times 5 \tag{6}$$

**BED and EUBED calculations**

Structures, plans, and dose matrices of single treatments for all patients were extracted from TPS and DICOM. BED using standard linear quadratic (LQ) modes was calculated as follows [32], with each voxel of the dose matrix converted into BED.

$$BED_i = D_i \left( 1 + \frac{D_i}{\alpha/\beta} \right) \tag{7}$$

Where  $D_i$  is the total dose delivered to the individual voxel.  $\alpha/\beta = 10 \text{ Gy}$  for tumor and  $\alpha/\beta = 3 \text{ Gy}$  for OARs.

The EUBED concept more accurately describes the role of radiobiological effects caused by dose non-uniformity in clinical outcomes. In this study, EUBED was calculated as follows [33]:

$$EUBED = -\frac{1}{\alpha} \ln \left( \sum_{i=1}^N v_i e^{-\alpha \cdot BED_i} \right) \tag{8}$$

Where  $v_i$  is the fractional normalized volume in the DVH or the ratio  $N_i/N$ ,  $N_i$  is the number of voxels receiving the same dose, and  $\alpha$  is 0.3 [33].

**Table 2.** Parameters used for TCP and NTCP calculations

Tissue	Complication	TD <sub>50</sub> (Gy)	α/β (Gy)	α	γ <sub>50</sub>
Tumor	–	70	10	–10	3
Bladder	Hematuria	80	3	2	4
Rectum	Hemorrhage	80	3	8.33	4
Intestines	Intestinal fistula	55	3	6	4

**Statistical analysis**

SPSS v. 26.0 software (IBM, Armonk, NY, USA) was used for statistical analyses. Data were presented as mean ± standard deviation ( $\bar{x} \pm S$ ). Evaluation parameters of each group, which conformed to a normal distribution as determined through normality testing, were conducted using a matched samples *t*-test. Test methods of TCP and NTCP were different because dosimetric differences did not follow a linear relationship, and the data were not normally distributed. A non-parametric Friedman test was then conducted [34, 35]. However, non-parametric Wilcoxon rank test

was applied for post-hoc multiple comparisons in cases when the assumptions in Friedman test were rejected ( $p < 0.05$ ). *P*-value  $< 0.05$  indicated statistically significant differences.

**Results**

**Isodose line**

Figure 1 shows an image of a representative case from the patient cohort. The 9 Gy isodose line (high-dose region) of HIPO1 was smoother than that of IPSA and HIPO2, especially in the cervix region.

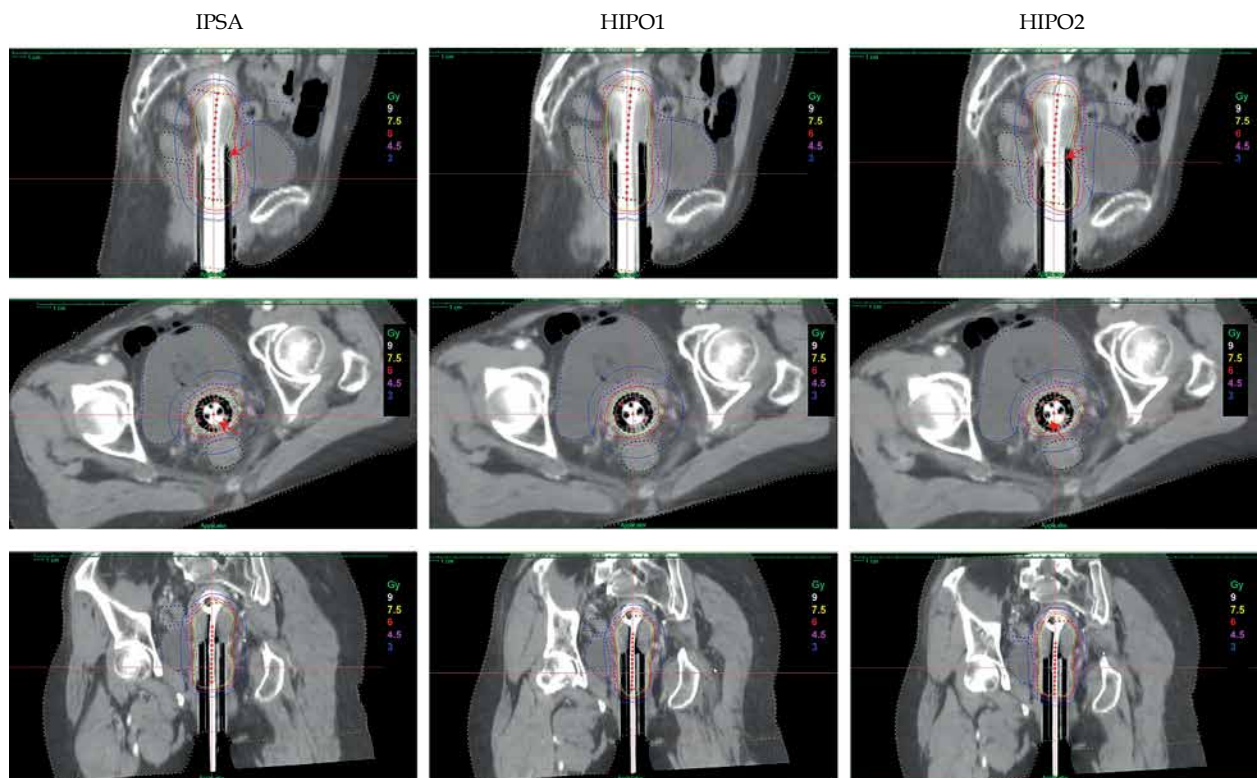


**Fig. 1.** Isodose lines of the same patient under three optimized conditions calculated by IPSA, HIPO1, and HIPO2 in the sagittal, axial, and coronal planes. Arrows indicate the 9 Gy isodose line (high-dose region)

**Table 3.** Comparison of physical parameters of IPSA, HIPO1, and HIPO2 plans

	Parameter	IPSA	HIPO1	$p_1$	HIPO2	$p_2$	$p_3$
CTV	D <sub>100</sub> (Gy)	3.00 ±0.45	3.25 ±0.31	0.001	3.28 ±0.37	0.006	0.536
	V <sub>150%</sub> (%)	52.91 ±3.24	55.33 ±2.81	≤ 0.001	53.58 ±3.49	0.310	0.001
	V <sub>200%</sub> (%)	28.92 ±3.36	34.27 ±2.81	≤ 0.001	29.41 ±3.90	0.448	≤ 0.001
	HI	0.41 ±0.03	0.39 ±0.03	≤ 0.001	0.40 ±0.04	0.310	0.001
	CI	0.79 ±0.06	0.80 ±0.07	0.124	0.82 ±0.07	≤ 0.001	0.002
Bladder	D <sub>1cc</sub> (Gy)	4.80 ±0.34	5.06 ±0.30	≤ 0.001	4.72 ±0.33	0.098	≤ 0.001
	D <sub>2cc</sub> (Gy)	4.59 ±0.32	4.77 ±0.28	≤ 0.001	4.47 ±0.29	0.004	≤ 0.001
Rectum	D <sub>1cc</sub> (Gy)	4.61 ±0.61	4.79 ±0.64	0.001	4.50 ±0.61	0.078	≤ 0.001
	D <sub>2cc</sub> (Gy)	4.26 ±0.64	4.37 ±0.66	0.015	4.11 ±0.63	0.010	≤ 0.001
Intestines	D <sub>1cc</sub> (Gy)	3.85 ±1.04	4.05 ±1.06	≤ 0.001	3.93 ±1.02	0.053	0.004
	D <sub>2cc</sub> (Gy)	3.51 ±1.04	3.67 ±1.02	≤ 0.001	3.57 ±1.00	0.065	0.001

CTV – clinical target volume, IPSA – inverse planning simulated annealing, HIPO – hybrid inverse planning optimization, HI – homogeneity index, CI – conformity index,  $p_1$  – represents *p*-value of IPSA vs. HIPO1;  $p_2$  – represents *p*-value of IPSA vs. HIPO2;  $p_3$  – represents *p*-value of HIPO1 vs. HIPO2

**Target and OARs doses**

The target volumes in the 32 patients were 43-156 cm<sup>3</sup> (median, 93 cm<sup>3</sup>). The difference in target dose among the three techniques is shown in Table 3. D<sub>100</sub> had no remarkable difference between HIPO1 and HIPO2 ( $p > 0.05$ ). V<sub>150%</sub> and V<sub>200%</sub> were higher in HIPO1 than in IPSA and HIPO2 (Figure 2) ( $p < 0.05$ ). However, V<sub>150%</sub> and V<sub>200%</sub> of IPSA and HIPO2 were similar ( $p > 0.05$ ). CI was higher in HIPO2 than those in IPSA and HIPO1 by 3.80% and 2.50%, respectively ( $p < 0.002$ ). However, HI was lower in HIPO1 than in HIPO2 and IPSA by about 2.50-4.88%.

D<sub>1cc</sub> and D<sub>2cc</sub> of OARs were highest in HIPO1 than those in IPSA and HIPO2. The doses of D<sub>2cc</sub> to the bladder and rectum were lowest in HIPO2 than in of IPSA and HIPO1. Also, the average values of D<sub>1cc</sub> of OARs were similar between IPSA and HIPO2.

**Results of radiobiological model**

EUBED: The comparison average results of EUBEDs among the three plans are shown in Table 4. IPSA had the lowest EUBED of HR-CTV (12.27 ± 0.28 Gy) than in HIPO1 and HIPO2. EUBED in HR-CTV was similar between HIPO1 and HIPO2 ( $p > 0.05$ ). HIPO2 had the lowest EUBEDs of the

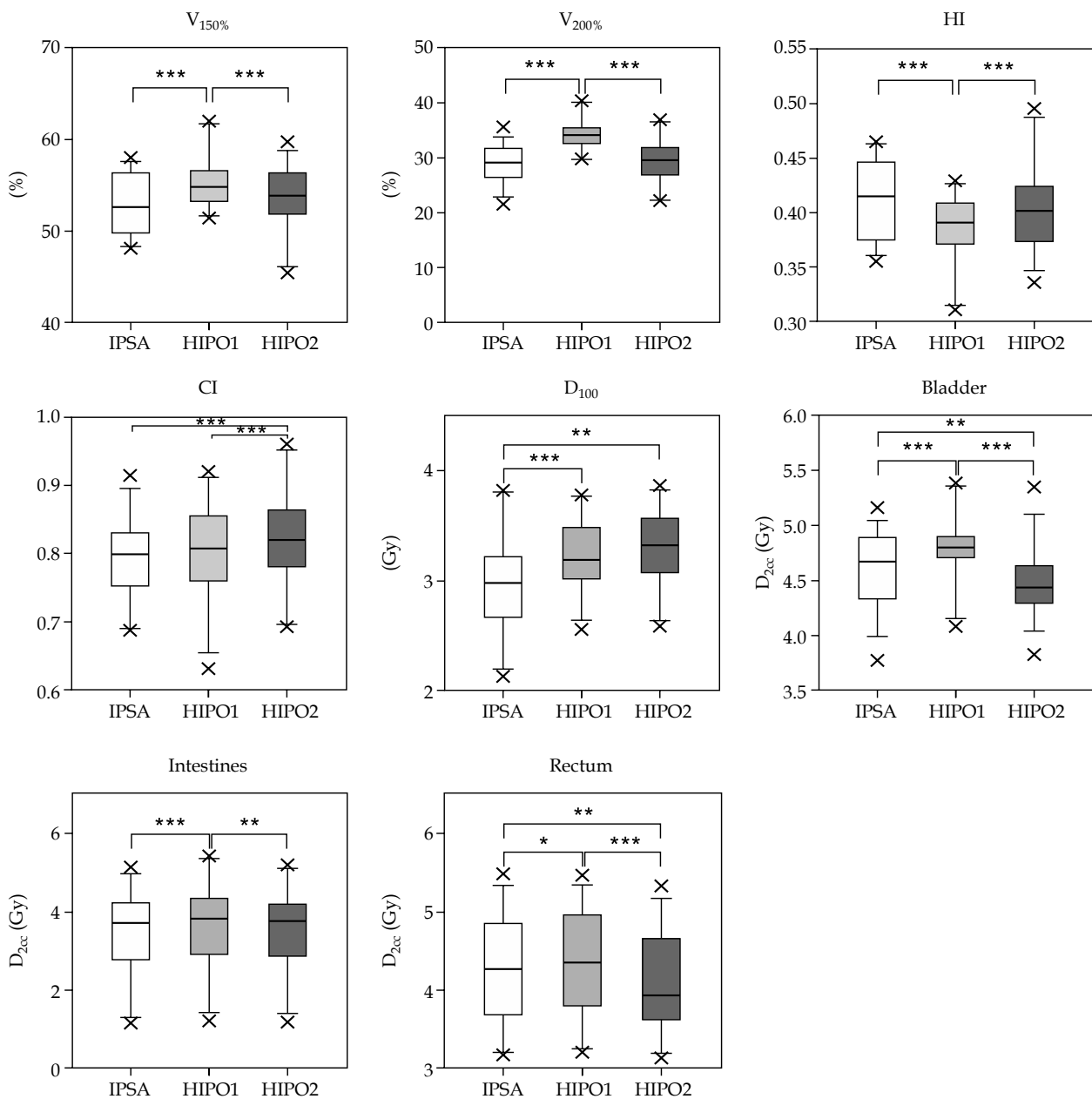


**Fig. 2.** Main dosimetric parameters of IPSA, HIPO1, and HIPO2 (D<sub>2cc</sub> of the bladder, rectum, and intestines; D<sub>100</sub>, V<sub>150%</sub>, V<sub>200%</sub>, HI, and CI) were analyzed via box method. Asterisk (\*) indicates that the corresponding p-value is between 0.01 and 0.05. Two asterisks (\*\*) indicate that the corresponding p-value is between 0.001 and 0.01. Three asterisks (\*\*\*) indicate that the corresponding p-value is less than or equal to 0.001

**Table 4.** Comparison of EUBED among IPSA, HIPO1, and HIPO2

Observation indexes	IPSA	HIPO1	$p_1$	HIPO2	$p_2$	$p_3$
HR-CTV (Gy)	12.27 ±0.28	12.47 ±0.18	≤ 0.001	12.44 ±0.24	≤ 0.001	0.359
Bladder (Gy)	2.54 ±0.49	2.61 ±0.50	≤ 0.001	2.46 ±0.45	≤ 0.001	≤ 0.001
Rectum (Gy)	4.20 ±1.17	4.36 ±1.32	0.012	4.03 ±1.11	0.025	≤ 0.001
Intestines (Gy)	1.56 ±0.52	1.65 ±0.56	≤ 0.001	1.59 ±0.55	0.031	≤ 0.001

IPSA – inverse planning simulated annealing, HIPO – hybrid inverse planning optimization,  $p_1$  – represents p-value of IPSA vs. HIPO1,  $p_2$  – represents p-value of IPSA vs. HIPO2,  $p_3$  – represents p-value of HIPO1 vs. HIPO2

**Table 5.** Comparison of TCP and NTCP among IPSA, HIPO1, and HIPO2 (median, quartile)

Parameter	IPSA	HIPO1	HIPO2	p-value (Friedman) <sup>a</sup>	p-value (Wilcoxon) <sup>b</sup>
TCP (%)	92.39 (90.80-94.30)	92.95 (90.95-93.96)	93.18 (91.39-94.74)	0.123	HIPO1-HIPO2: 0.003
NTCP <sub>bladder</sub> (%)	0.23 (0.14-0.31)	0.24 (0.16-0.33)	0.20 (0.14-0.25)	≤ 0.001	IPSA-HIPO1: 0.037 IPSA-HIPO2: 0.001 HIPO1-HIPO2: ≤ 0.001
NTCP <sub>rectum</sub> (%)	1.62 (0.92-3.07)	2.15 (0.98-4.28)	1.24 (0.66-2.55)	≤ 0.001	IPSA-HIPO1: 0.001 HIPO1-HIPO2: ≤ 0.001
NTCP <sub>intestines</sub> (%)	24.50 (16.22-33.76)	26.79 (17.73-41.98)	26.45 (16.97-37.59)	0.001	IPSA-HIPO1: ≤ 0.001

<sup>a</sup> Non-parametric Friedman test among the three groups; <sup>b</sup> Non-parametric Wilcoxon rank test was used for post-hoc analysis of differences between two groups

bladder and rectum compared with IPSA and HIPO1. Furthermore, EUBEDs of the bladder, rectum, and intestines were highest in HIPO1 than in IPSA and HIPO2.

TCP and NTCP: TCPs found no remarkable difference between IPSA and HIPO1 (Table 5). NTCPs of OARs were lower in IPSA than in HIPO1 by 4.17% (bladder), 24.65% (rectum), and 8.55% (intestines). Moreover, TCPs found no remarkable difference between IPSA and HIPO2. NTCP of the bladder was lower in HIPO2 than in IPSA by 13.04%. TCP was higher in HIPO2 compared with HIPO1 by 0.23%. NTCPs of the bladder and rectum were lower in HIPO2 than in HIPO1 by 16.67% and 42.33%, respectively.

## Discussion

Brachytherapy plays an essential role in cervical cancer treatment, and IPSA is widely used in BT. However, HIPO has also been introduced into BT [36]. DTDC and DTGR are used to modulate the dwell-time distribution in IPSA and HIPO, respectively. Furthermore, IPSA and HIPO have different operating principles [37, 38]. For example, the DTDC parameter in IPSA defines an upper limit of dwell time, which controls the dwell-time change between adjacent dwell locations in each catheter while the DTGR parameter of HIPO is a dwell-time-gradient constraint that limits the large time fluctuation in the adjoining dwell location. A previous study suggested that the DTDC value should be about 0.6 in ICBT if OARs' doses are limited for patients with radical cervical cancer [39]. Although DTDC and DTGR have different operating principles, the range of both DTDC and DTGR is 0-1. Therefore, taking the same value in the range of 0-1 has similar modification effect; therefore, the DTDC and DTGR values were both set at 0.6 in this study.

Herein, various radiobiological metrics were established to assess the correlation between radiation dose

and biological effects for better clinical practice. EUD can be used to calculate TCP and NTCP of non-uniform dose distribution. Other models, such as Lyman-Kutcher-Burman (LKB) [40] or relative seriality (RS) [41] models have the proper formulations to accommodate this need as well. In this study, Niemierko's model was selected because it is simple and convenient for calculation, and is recommended for BT in the AAPM Report 137. Chow *et al.* [42] retrospectively analyzed the range of fixed parameters used in BED model, which are caused by individual differences in patients. Several other researchers studying squamous cell carcinoma have also reported the range of these parameters. In this study,  $\alpha$  and  $\alpha/\beta$  were 0.3 Gy<sup>-1</sup> (0.06 ~ 0.74 Gy<sup>-1</sup>) and 10 Gy (5.9 ~ 76.9 Gy), respectively. Furthermore, the median values were used for data comparison since the study was conducted based on a single treatment. The  $\alpha/\beta$  ratio for all OARs was 3 Gy.

The current study has some limitations. This study mainly aimed to compare the differences of physical and radiobiological doses between different optimization methods in a single IC/ISBT fraction. However, all EBRT and the other four BTs in the total treatment were unified and simplified. Also, the adjustment of optimization parameters is subjective, and it largely depends on dosimetrist/physicist experience.

Human biological information is complex and diverse. Therefore, a comparative trial should be further carried out to obtain a higher level of clinical evidence. Although the statistical results can provide a reference for clinical radiotherapy workers, a more in-depth research is needed to solve the influence on those radiobiological factors.

## Conclusions

Although the two inverse optimization algorithms meet clinical needs in cervical cancer treatment through

combined ICBT/ISBT, HIPO2 (with an unlocked uterine tube) provides better dose conformability and lower NTCP. Therefore, HIPO2 is recommended as an optimization algorithm in IC/ISBT of cervical cancer.

### Acknowledgements

This study was in part funded by a research grant (No.: 2021-DF-016) of Elekta AB (Stockholm, Sweden). The funders had no role in study design, data collection, and analysis, and decisions on preparation of the manuscript. This study was partially supported by Sichuan Science and Technology Program (No.: 2022YFG0194, 2022YFS0047, 2021YFG0320, 2020YJ0446) and Medical Engineering Innovation Fund for Cancer (No. ZYGX-2021YGCX002).

### Disclosure

The authors report no conflict of interest.

### References

1. Taggar AS, Damato AL, Cohen GN et al. Brachytherapy. In: Chang EL, Brown PD, Lo SS et al. (Eds.). *Adult CNS Radiation Oncology: Principles and Practice*. Springer International Publishing, Cham 2018; 723-744.
2. He R, Zhu B, Liu J et al. Women's cancers in China: a spatio-temporal epidemiology analysis. *BMC Womens Health* 2021;21: 116.
3. Guinot JL, Perez-Calatayud J, Van Limbergen EJS. The GEC-ESTRO Handbook of Brachytherapy. 2017.
4. Van der Walt HC. Development of a brachytherapy treatment planning module for cervix cancer utilising biological dose metrics. University of the Free State, 2020.
5. Wang X, Wang P, Tang B et al. An inverse dose optimization algorithm for three-dimensional brachytherapy. *Front Oncol* 2020; 10: 564580.
6. Jamema SV, Sharma S, Mahantshetty U et al. Comparison of IPSA with dose-point optimization and manual optimization for interstitial template brachytherapy for gynecologic cancers. *Brachytherapy* 2011; 10: 306-312.
7. Palmqvist T, Dybdahl Wanderås A, Langeland Marthinsen AB et al. Dosimetric evaluation of manually and inversely optimized treatment planning for high dose rate brachytherapy of cervical cancer. *Acta Oncol* 2014; 53: 1012-1018.
8. Kannan RA, Gururajachar JM, Ponni A et al. Comparison of manual and inverse optimisation techniques in high dose rate intracavitary brachytherapy of cervical cancer: A dosimetric study. *Rep Pract Oncol Radiother* 2015; 20: 365-369.
9. Kim DH, Wang-Chesebro A, Weinberg V et al. High-dose rate brachytherapy using inverse planning simulated annealing for locoregionally advanced cervical cancer: a clinical report with 2-year follow-up. *Int J Radiat Oncol Biol Phys* 2009; 75: 1329-1334.
10. Tinkle CL, Weinberg V, Chen LM et al. Inverse planned high-dose-rate brachytherapy for locoregionally advanced cervical cancer: 4-year outcomes. *Int J Radiat Oncol Biol Phys* 2015; 92: 1093-1100.
11. Panettieri V, Smith RL, Mason NJ et al. Comparison of IPSA and HIPO inverse planning optimization algorithms for prostate HDR brachytherapy. *J Appl Clin Med Phys* 2014; 15: 5055.
12. Poulthier E, Varfalvy N, Aubin S et al. Comparison of dose and catheter optimization algorithms in prostate high-dose-rate brachytherapy. *Brachytherapy* 2016; 15: 102-111.
13. Choi CH, Park SY, Park JM et al. Comparison of the IPSA and HIPO algorithms for interstitial tongue high-dose-rate brachytherapy. *PLoS One* 2018; 13: 205-229.
14. Trnková P, Baltas D, Karabis A et al. A detailed dosimetric comparison between manual and inverse plans in HDR intracavitary/interstitial cervical cancer brachytherapy. *J Contemp Brachytherapy* 2010; 2: 163-170.
15. Fu Q, Xu Y, Zuo J et al. Comparison of two inverse planning algorithms for cervical cancer brachytherapy. *J Appl Clin Med Phys* 2021; 22: 157-165.
16. Bhatla N, Berek JS, Cuello Fredes M et al. Revised FIGO staging for carcinoma of the cervix uteri. *Int J Gynaecol Obstet* 2019; 145: 129-135.
17. Report 89. *JICRU* 2013;13: NP.
18. Liu M, Wang X, Yuan K et al. A verification study of offset values of different applicators in afterloading brachytherapy. *Chinese J Radiat Oncol* 2020; 29: 126-130.
19. Chajon E, Dumas I, Touleimat M, et al. Inverse planning approach for 3-D MRI-based pulse-dose rate intracavitary brachytherapy in cervix cancer. *Int J Radiat Oncol Biol Phys* 2007; 69: 955-961.
20. Kubicky CD, Yeh BM, Lessard E et al. Inverse planning simulated annealing for magnetic resonance imaging-based intracavitary high-dose-rate brachytherapy for cervical cancer. *Brachytherapy* 2008; 7: 242-247.
21. Lessard E, Hsu IC, Pouliot J. Inverse planning for interstitial gynecologic template brachytherapy: truly anatomy-based planning. *Int J Radiat Oncol Biol Phys* 2002;54: 1243-1251.
22. Lessard E, Pouliot J. Inverse planning anatomy-based dose optimization for HDR-brachytherapy of the prostate using fast simulated annealing algorithm and dedicated objective function. *Med Phys* 2001; 28: 773-779.
23. Karabis A, Giannouli S, Baltas DJR et al. 40 HIPO: a hybrid inverse treatment planning optimization algorithm in HDR brachytherapy. *Radiother Oncol* 2005; 76: S29.
24. Wu A, Ulin K, Sternick ES. A dose homogeneity index for evaluating 192Ir interstitial breast implants. *Med Phys* 1988; 15: 104-107.
25. Baltas D, Kolotas C, Geramani K et al. A conformal index (COIN) to evaluate implant quality and dose specification in brachytherapy. *Int J Radiat Oncol Biol Phys* 1998; 40: 515-524.
26. Niemierko AJMP. A generalized concept of equivalent uniform dose (EUD). *Med Phys* 1999; 26: 1100.
27. Niemierko A. A unified model of tissue response to radiation. Proceedings of the 41th AAPM annual meeting. 1100. Nashville: Wikipedia, 1999.
28. Oinam AS, Singh L, Shukla A et al. Dose volume histogram analysis and comparison of different radiobiological models using in-house developed software. *J Med Phys* 2011; 36: 220-229.
29. Gay HA, Niemierko A. A free program for calculating EUD-based NTCP and TCP in external beam radiotherapy. *Phys Med* 2007; 23: 115-125.
30. Wu Q, Mohan R, Niemierko A et al. Optimization of intensity-modulated radiotherapy plans based on the equivalent uniform dose. *Int J Radiat Oncol Biol Phys* 2002; 52: 224-235.
31. Nesvacil N, Tanderup K, Lindegaard JC et al. Can reduction of uncertainties in cervix cancer brachytherapy potentially improve clinical outcome? *Radiother Oncol* 2016; 120: 390-396.
32. McMahon SJ. The linear quadratic model: usage, interpretation and challenges. *Phys Med Biol* 2018; 64: 01tr01.
33. Fields EC, Melvani R, Hajdok G et al. A multi-institution, retrospective analysis of cervix intracavitary brachytherapy treatments. Part 1: Is EQD2 good enough for reporting radiobiological effects? *Int J Radiat Oncol Biol Phys* 2017; 99: 219-226.
34. Fröhlich G, Geszti G, Vizkeleti J et al. Dosimetric comparison of inverse optimisation methods versus forward optimisa-

- tion in HDR brachytherapy of breast, cervical and prostate cancer. *Strahlenther Onkol* 2019; 195: 991-1000.
35. Dinkla AM, van der Laarse R, Kaljouw E et al. A comparison of inverse optimization algorithms for HDR/PDR prostate brachytherapy treatment planning. *Brachytherapy* 2015; 14: 279-288.
  36. Pokharel S, Rana S, Blikenstaff J et al. Evaluation of hybrid inverse planning and optimization (HIPO) algorithm for optimization in real-time, high-dose-rate (HDR) brachytherapy for prostate. *J Appl Clin Med Phys* 2013; 14: 4198.
  37. Smith RL, Panettieri V, Lancaster C et al. The influence of the dwell time deviation constraint (DTDC) parameter on dosimetry with IPSA optimisation for HDR prostate brachytherapy. *Australas Phys Eng Sci Med* 2015; 38: 55-61.
  38. Mavroidis P, Katsilieri Z, Kefala V et al. Radiobiological evaluation of the influence of dwell time modulation restriction in HIPO optimized HDR prostate brachytherapy implants. *J Contemp Brachytherapy* 2010; 2: 117-128.
  39. Yan G, Kang S, Tang B et al. Effect of the dwell time deviation constraint on brachytherapy treatment planning for cervical cancer. *J Int Med Res* 2021; 49: 3000605211037477.
  40. Lyman JT. Complication probability as assessed from dose-volume histograms. *Radiat Res Suppl* 1985; 8: S13-19.
  41. Källman P, Agren A, Brahme A. Tumour and normal tissue responses to fractionated non-uniform dose delivery. *Int J Radiat Biol* 1992; 62: 249-262.
  42. Chow B, Warkentin B, Menon G. Radiobiological dose calculation parameters for cervix cancer brachytherapy: A systematic review. *Brachytherapy* 2019; 18: 546-558.